

# Measurement of the nuclear magnetic moments of $^{57}\text{Ni}$ and $^{59}\text{Fe}$

T. Ohtsubo, D. J. Cho, Y. Yanagihashi, and S. Ohya  
*Department of Physics, Niigata University, Niigata 950-21, Japan*

S. Muto  
*National Laboratory for High Energy Physics, Tsukuba 350, Japan*  
 (Received 19 January 1996)

The magnetic hyperfine splitting frequencies of (i)  $^{57}\text{Ni}$  in Fe ( $^{57}\text{NiFe}$ ), (ii)  $^{57}\text{Ni}$  in Ni ( $^{57}\text{NiNi}$ ), and (iii)  $^{59}\text{Fe}$  in Fe ( $^{59}\text{FeFe}$ ) were measured with the technique of nuclear magnetic resonance on oriented nuclei (NMR-ON) at low temperatures. The NMR-ON spectra were observed by detecting the  $\beta$ -ray asymmetries. The resonance frequencies at zero external magnetic field were deduced from the extrapolation of the external field dependence of the resonance frequencies:  $\nu(^{57}\text{NiFe})=94.23(2)$  MHz,  $\nu(^{57}\text{NiNi})=30.02(4)$  MHz, and  $\nu(^{59}\text{FeFe})=57.719(11)$  MHz. With the known hyperfine fields of  $B_{\text{HF}}(\text{NiNi})=-7.406(8)$  T and  $B_{\text{HF}}(\text{FeFe})=-33.82(3)$  T, the magnetic moments of  $^{57}\text{Ni}$  and  $^{59}\text{Fe}$  were determined to be  $\mu(^{57}\text{Ni})=-0.7975(14)\mu_N$  and  $\mu(^{59}\text{Fe})=-0.3358(4)\mu_N$ . The precise value of the hyperfine field of  $B_{\text{HF}}(^{57}\text{NiFe})$  was also deduced as  $-23.25(5)$  T. The measured values of the magnetic moment are compared with those based on the shell model. [S0556-2813(96)00808-4]

PACS number(s): 21.10.Ky, 76.60.-k

## I. INTRODUCTION

The nuclear magnetic moment is a good probe for studying nuclear structure. The electromagnetic properties of nuclei that are doubly closed-shell plus or minus one nucleon are expected to be well described by the simple independent-particle model. Near the  $jj$ -closed-shell nuclei, the deviations of the magnetic moments from the single-particle values (Schmidt values) are mainly caused by  $I^\pi=1^+$  core polarization [1] and by mesonic exchange currents [2]. Systematic study of the electromagnetic moments in the vicinity of the doubly closed shell nuclei provides detailed information on these effects. Recently, van der Merwe *et al.* [3] studied the effective interactions in the  $0f1p$ -shell region. They derived the effective interaction by fitting energy levels in this region and calculated the electromagnetic moments. To study the magnetic moments in this region, we have applied the technique of nuclear magnetic resonance on oriented nuclei (NMR-ON) to  $^{57}\text{Ni}$  and  $^{59}\text{Fe}$ .

Using the low-temperature nuclear orientation method, the magnetic moments of  $^{57}\text{Ni}$  and  $^{59}\text{Fe}$  have been previously measured to be  $0.88(6)\mu_N$  [4] and  $0.29(3)\mu_N$ , [5] respectively. Although the temperatures in these measurements were very low (3–20 mK), the  $\gamma$ -ray anisotropies following the decay of oriented nuclei were too small to determine the magnetic moments with high accuracy. The small anisotropies of  $\gamma$  rays are mainly due to the small deorientation parameter  $U_2$  and small directional correlation coefficient  $A_2$ . On the other hand, the asymmetry of  $\beta$  rays from these nuclei is expected to be large enough to observe the NMR effect. The sign of the magnetic moment can be also determined from this anisotropy, which cannot be done with  $\gamma$  rays.

Because the technique of NMR-ON provides accurate values of magnetic hyperfine splitting, it gives us not only the value of the magnetic moment but also information on the environment of extreme dilute impurity nuclei in a ferro-

magnetic host [6]. This is the first experiment of NMR-ON for Ni and Fe isotopes. The  $^{57}\text{Ni}$  and  $^{59}\text{Fe}$  isotopes can be very important probes in the study of ferromagnetic alloys.

## II. PRINCIPLE

The  $^{57}\text{Ni}$  and  $^{59}\text{Fe}$  decay schemes are shown in Fig. 1. The highest energies of  $\beta$  rays of interest are 865 keV for  $^{57}\text{Ni}$  and 466 keV for  $^{59}\text{Fe}$ . The angular distribution of  $\beta$

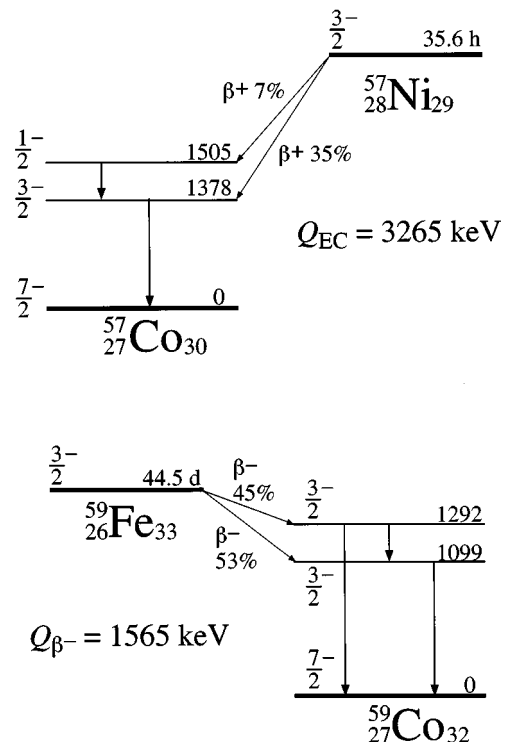


FIG. 1. Partial decay schemes of  $^{57}\text{Ni}$  and  $^{59}\text{Fe}$ .

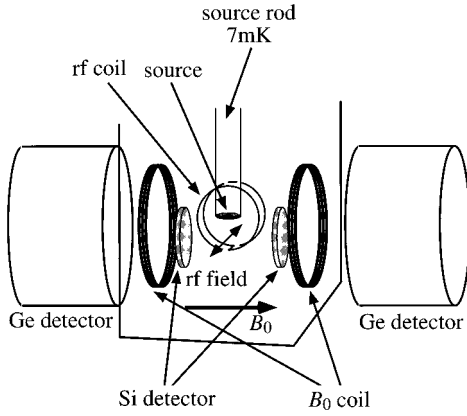


FIG. 2. Schematic view of arrangement of Si detectors.

rays from oriented nuclei is described as [7]

$$W(\theta) = \sum_{\lambda} B_{\lambda} A_{\lambda} P_{\lambda}(\cos \theta),$$

where  $\theta$  is the angle between the orientation axis and emitted  $\beta$  ray,  $B_{\lambda}$  are the orientation parameters,  $A_{\lambda}$  are the  $\beta$  angular distribution coefficients, and  $P_{\lambda}$  are the Legendre polynomials. In the current cases, only  $\lambda = 0, 1$  terms are present. Therefore

$$W(\theta) = 1 + B_1 A_1 \cos \theta.$$

The ratio of  $\beta$ -ray counts,  $R$ , at  $0^\circ$  and  $180^\circ$  relative to the orientation axis is described as

$$R = \frac{N(0^\circ)}{N(180^\circ)} = \varepsilon \frac{(1 + B_1 A_1)}{(1 - B_1 A_1)}.$$

Here  $\varepsilon$  is the geometrical asymmetry of the  $\beta$ -ray detection system. If the orientation is destroyed by the applied radio-frequency (rf) field at the resonance frequency, the resonance is detected by the change of the ratio  $R$ .

### III. EXPERIMENTAL PROCEDURES

Sources of  $^{57}\text{Ni}$  were prepared by the recoil implantation method. Stacks of pure Ni and Fe foils (thickness  $\sim 1.5 \mu\text{m}$ ) were irradiated for 20 h with a 50-MeV  $\alpha$  beam (intensity  $\sim 1.5 \mu\text{A}$ ) from the SF cyclotron at the INS of University of Tokyo. The target was water cooled. Sources of  $^{59}\text{Fe}$  were prepared by neutron irradiation of Fe foils. Disks of 4 mm diameter,  $\sim 3 \mu\text{m}$  thick, pure (99.99%) Fe foils were irradiated with a thermal neutron flux of  $2.9 \times 10^{13}/\text{cm}^2 \text{ s}$  for 12 d in the reactor at the Japan Atomic Energy Research Institute. After irradiation, the samples were annealed at  $800^\circ\text{C}$  in a vacuum for 1 h. Then each sample was soldered to the cold finger of a  $^3\text{He}/^4\text{He}$  dilution refrigerator and was cooled down to about 7 mK. The temperatures of the  $^{57}\text{Ni}$  samples were monitored by  $^{56}\text{Co}$  which was produced simultaneously in the samples. As for the  $^{59}\text{Fe}$  samples, a  $^{54}\text{MnFe}$  thermometer was used.

The experimental setup of NMR-ON is shown in Fig. 2. The  $\beta$  rays were detected with two Si detectors of  $50 \text{ mm}^2$  area and 0.5 mm thickness at  $0^\circ$  and  $180^\circ$  with respect to the

orientation axis (the direction of the external magnetic field). The Si detectors were mounted on a heat shield of 0.7 K inside of the  $^3\text{He}/^4\text{He}$  dilution refrigerator. The distance from the center of the sample to the surface of the detectors was 8 mm. The Si detectors were placed at a slightly lower position than that of the sample (angle of about  $14^\circ$ ) to get a high efficiency. The Si detectors were connected with stainless coaxial cables (about 1.2 m) to the preamplifiers which were placed outside the refrigerator. The  $\gamma$  rays were detected with pure Ge detectors (30% and 25%) outside the refrigerator. These energy-spectrum data were transferred to a microcomputer and stored in the storage device of the server workstation through the network. An external magnetic field  $B_0$  was produced by superconducting coils to polarize the Fe or Ni foils. An rf oscillating field modulated at a rate of 300 Hz was applied perpendicular to  $B_0$ . The  $\beta$ - and  $\gamma$ -ray detection system and the rf system were controlled by a microcomputer.

## IV. RESULTS

### A. $^{57}\text{Ni}$

The  $\beta$ -ray spectrum from the  $^{57}\text{Ni}$  source contains components from contaminant activities but they are small ( $^{55}\text{Co}$  and  $^{56}\text{Co}$ ,  $< 30\%$ ). The continuous  $\beta$ -ray spectra were analyzed in several energy regions to search for the NMR-ON resonance. The resonance peak for  $^{57}\text{NiFe}$  was found at about 93.5 MHz for  $B_0 = 0.2$  T. The results of the resonance frequency for the several energy regions are in agreement within the uncertainties. Therefore, the following results of the resonance frequency are from the sum of the  $\beta$ -ray energy regions (120–1000 keV). Before taking precise resonance spectra, the effective relaxation time was measured by turning the frequency modulation (FM) signal on and off. The effective relaxation time was determined to be 260(10) s using a single-exponential fit. Detailed results of the effective relaxation times of  $^{57}\text{NiFe}$  and  $^{57}\text{NiNi}$  are described in Ref. [8]. The resonance spectra measured for  $B_0 = 0.1, 0.2,$  and  $0.4$  T are shown in Fig. 3. An interval of 200 s was taken in each step to allow for the spin-lattice relaxation. The solid curves in Fig. 3 are the results of a least-squares fit assuming a resonance with a Gaussian shape and linear background. The linewidths are 0.24(1), 0.24(1), and 0.34(1) MHz including the FM bandwidth of  $\pm 0.05$  MHz for  $B_0 = 0.1$  T,  $\pm 0.05$  MHz for  $B_0 = 0.2$  T, and  $\pm 0.1$  MHz for  $B_0 = 0.4$  T. From least-squares fits of the resonance frequencies vs the external magnetic fields, the following results were obtained:

$$\nu(^{57}\text{NiFe}, B_0 = 0) = 94.23(2) \text{ MHz}$$

and

$$\frac{d\nu}{dB_0} (^{57}\text{NiFe}) = -3.89(11) \text{ MHz/T}.$$

The resonance spectra were also measured for  $^{57}\text{NiNi}$ . Those for  $B_0 = 0.1, 0.2,$  and  $0.4$  T are shown in Fig. 4. An interval of 200 s was taken in each step to allow for the effective spin-lattice relaxation time of 30(5) s [8]. The linewidths are 0.20(2), 0.26(1), and 0.26(1) MHz for

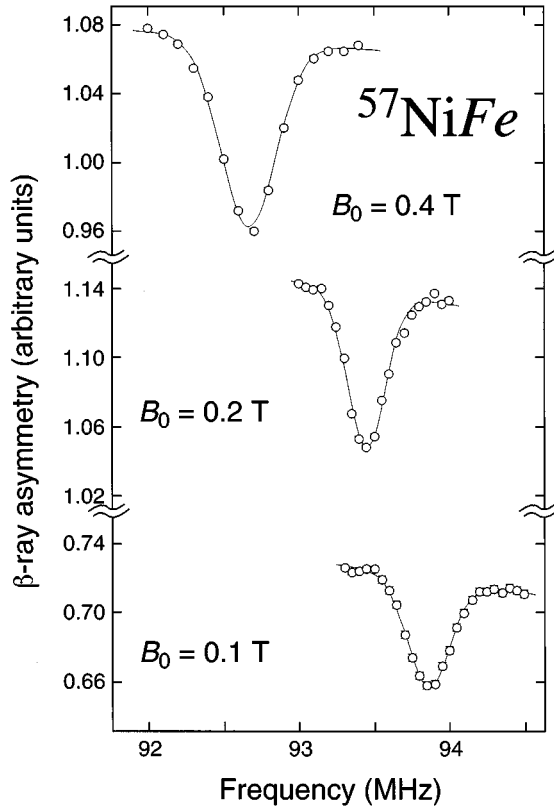


FIG. 3.  $\beta$ -NMR-ON spectra of  $^{57}\text{Ni}$  in Fe for three different magnetic fields. The  $\beta$ -ray asymmetry  $N(0^\circ)/N(180^\circ)$  is with respect to the orientation axis (the direction of the external magnetic field).

$B_0=0.1, 0.2,$  and  $0.4$  T, respectively, including the FM bandwidth of  $\pm 0.1$  MHz. From least-squares fits of the resonance frequencies vs the external magnetic fields, the following results were obtained:

$$\nu(^{57}\text{NiNi}, B_0=0) = 30.02(4) \text{ MHz}$$

and

$$\frac{d\nu}{dB_0}(^{57}\text{NiNi}) = -3.94(14) \text{ MHz/T.}$$

### B. $^{59}\text{Fe}$

In the  $^{59}\text{FeFe}$  sample, no contaminant  $\beta$ -decay activities are found from the analysis of the  $\gamma$ -ray spectrum. The resonance spectra were measured at  $B_0=0.1, 0.2,$  and  $0.4$  T as shown in Fig. 5. The FM bandwidth was  $\pm 0.02$  MHz. The effective relaxation time was obtained as  $16.7(33)$  ns at  $B_0=0.2$  T [8]. An interval of 25 ns was taken in each step to allow for the effective spin-lattice relaxation. The linewidths are  $0.072(6), 0.080(6),$  and  $0.072(8)$  MHz for  $B_0=0.1, 0.2,$  and  $0.4$  T, respectively including the FM bandwidth of  $\pm 0.02$  MHz. From least-squares fits of the resonance frequencies vs the external magnetic fields, the following results were obtained:

$$\nu(^{59}\text{FeFe}, B_0=0) = 57.719(11) \text{ MHz}$$

and

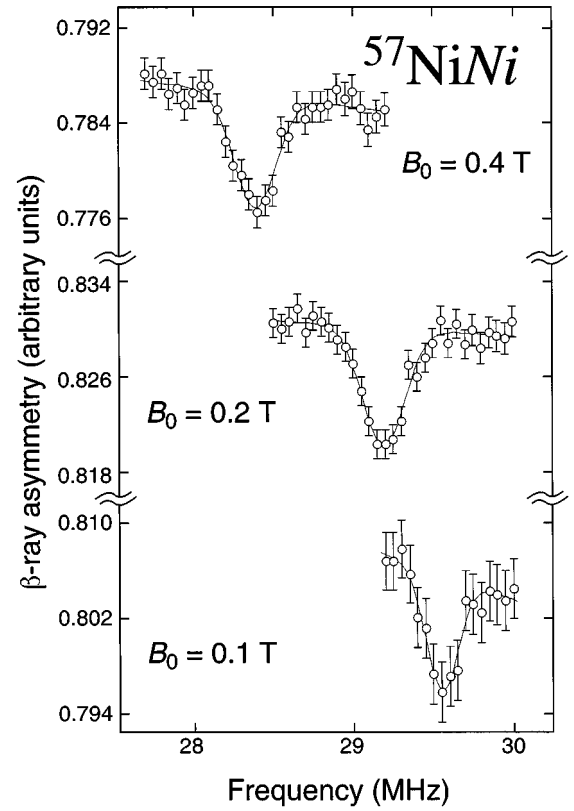


FIG. 4.  $\beta$ -NMR-ON spectra of  $^{57}\text{Ni}$  in Ni. See caption for Fig. 3.

$$\frac{d\nu}{dB_0}(^{59}\text{FeFe}) = -1.65(7) \text{ MHz/T.}$$

## V. DISCUSSION

### A. Magnetic moment of $^{57}\text{Ni}$ and the hyperfine field of NiFe

For a pure magnetic interaction, the resonance frequency is given by

$$\nu = |g(B_{\text{HF}} + (1+K)B_0)|\mu_N/h$$

and

$$\frac{d\nu}{dB_0} = \text{sgn}(B_{\text{HF}})|g(1+K)|\mu_N/h,$$

where  $g$  is the nuclear  $g$  factor,  $B_{\text{HF}}$  is the magnetic hyperfine field, and  $K$  is the Knight shift. The hyperfine field of Ni in Fe was reported to be  $|B_{\text{HF}}(\text{NiFe})| = 23.4(2)$  T by Mössbauer spectroscopy at liquid He temperatures [9]. The value of  $B_{\text{HF}}(\text{NiNi})$  was reported to be  $-7.406(8)$  T by the NMR method at liquid He temperatures [10]. Neglecting possible hyperfine anomalies, the magnetic moment of  $^{57}\text{Ni}$  and Knight shift factors  $K$  were deduced as

$$\mu(^{57}\text{Ni}, \frac{3}{2}^-; \text{NiFe}) = -0.792(7) \mu_N,$$

$$K(\text{NiFe}) = -3.4(29) \times 10^{-2},$$

$$\mu(^{57}\text{Ni}, \frac{3}{2}^-; \text{NiNi}) = -0.7977(14) \mu_N,$$

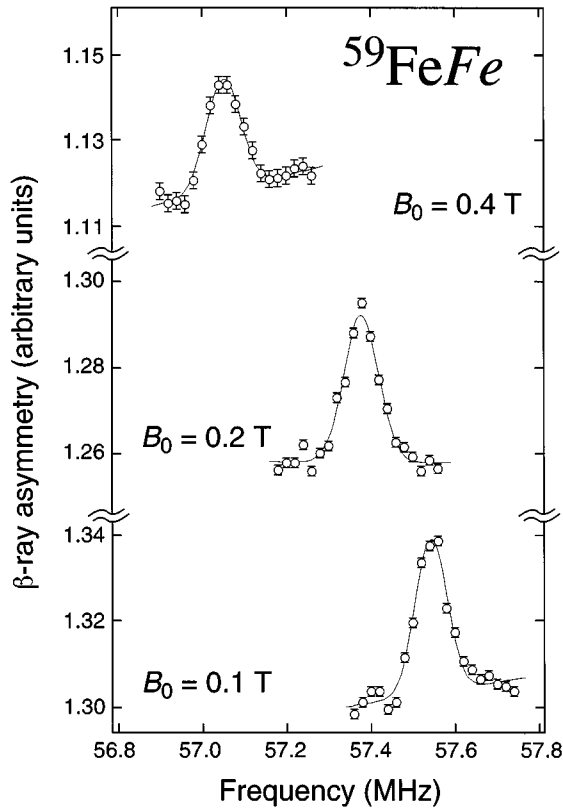


FIG. 5.  $\beta$ -NMR-ON spectra of  $^{59}\text{Fe}$  in Fe. See caption for Fig. 3.

$$K(\text{NiNi}) = -2.8(35) \times 10^{-2},$$

and

$$\text{weighted average of } \mu(^{57}\text{Ni}, \frac{3}{2}^-) = -0.7975(14) \mu_N.$$

The negative sign of the magnetic moment of  $^{57}\text{Ni}$  was deduced from the sign of the  $\beta$  asymmetry destruction on resonance as shown in Fig. 4 and the sign of the hyperfine field of  $B_{\text{HF}}(\text{NiNi})$ . The current precise value is slightly in disagreement with the previous value of  $(-0.88(6) \mu_N$ .

The main part of the uncertainty in  $\mu(^{57}\text{Ni}; \text{NiFe})$  is due to the uncertainty in the hyperfine field of  $B_{\text{HF}}(\text{NiFe})$ . We deduced a more precise value of  $B_{\text{HF}}(\text{NiFe})$  using our value of  $\mu(^{57}\text{Ni}; \text{NiNi})$  as

$$B_{\text{HF}}(\text{NiFe}) = -23.25(4) \text{ T}.$$

For the Ni isotopes the magnetic moment of the  $\frac{3}{2}^-$  state is known to be  $-0.7502(2) \mu_N$  for  $^{61}\text{Ni}$  [11] in addition to the current result of  $\mu(^{57}\text{Ni}) = -0.7977(14) \mu_N$ . The Schmidt value of the  $p_{3/2}$  neutron state is  $-1.91 \mu_N$ . The large deviation of the magnetic moment from the Schmidt value can be explained using the core-polarization formula [1]. With the neutron configurations of  $(f_{7/2})^8(p_{3/2})$  and  $(f_{7/2})^8(f_{5/2})^4(p_{3/2})$  for  $^{57}\text{Ni}$  and  $^{61}\text{Ni}$ , respectively, the calculated values are  $-1.15 \mu_N$  and  $-1.56 \mu_N$ , which are still in disagreement with the experimental values. The parameter set of the harmonic-oscillator potential with  $C = 35 \text{ MeV}$  was used in the calculation. With another configuration of  $(f_{7/2})^6(p_{3/2})^3$  and  $(f_{7/2})^8(f_{5/2})^2(p_{3/2})^3$  for  $^{57}\text{Ni}$  and  $^{61}\text{Ni}$ ,

respectively, the calculated values are  $-0.280 \mu_N$  and  $-0.322 \mu_N$ . The  $\frac{3}{2}^-$  states may be a mixture of the above configurations.

Glaudemans *et al.* [12] have calculated energy levels and moments of Ni isotopes using a  $^{56}\text{Ni}$  core and the five adjustable parameters fitted by the experimental data of Ni isotopes. The calculated magnetic moments are  $-0.9 \mu_N$  and  $-0.77 \mu_N$  for  $^{57}\text{Ni}$  and  $^{61}\text{Ni}$ , respectively, which are in good agreement with the experimental values.

Recently, van der Merwe *et al.* [3] have studied the effective interactions for  $fp$ -shell nuclei. They assumed a core of  $^{40}\text{Ca}$  and a model space up to a two-particle-one-hole ( $2p-1h$ ) configuration in  $fp$  shell for their shell-model basis. The effective interaction was derived by fitting two-body matrix elements to the energy levels in  $A = 41-66$  nuclei. They also calculated electromagnetic moments with their interactions. Agreements with the experimental values were reasonable except for some nuclei including  $^{57}\text{Ni}$ . The calculated value of the magnetic moment of  $^{57}\text{Ni}$  is  $\mu_{\text{theory}}(^{57}\text{Ni}; g_{\text{free}}) = -1.606 \mu_N$  with  $g_s(\text{free})$ . They also deduced the effective  $g$  factors [ $g_s(p) = 5.031$ ,  $g_s(n) = -3.041$ ,  $g_l(p) = 1$ ,  $g_l(n) = 0$ ] by fitting the experimental values. Even though these authors used effective  $g$  factors, there is a large discrepancy between the calculated value of  $\mu_{\text{theory}}(^{57}\text{Ni}; g_{\text{eff}}) = -1.274 \mu_N$  and the current experimental value of  $\mu(^{57}\text{Ni}) = -0.7977(14) \mu_N$ .

More recently, Semon *et al.* [13] measured absolute branching ratios for the  $\beta$  decay of  $^{57}\text{Cu}$  that is the mirror nucleus of  $^{57}\text{Ni}$ . Also, they calculated the magnetic moments of the mirror nuclei using the effective interaction [14] including configuration mixing up to  $3p-2h$  by adjusting the single-particle energy. The calculated value of  $^{57}\text{Ni}$  is  $-0.628 \mu_N$ . Moreover, including meson exchange current effects [15], they obtained  $-0.71 \mu_N$ , which is in better agreement with the current experimental value. For a more reliable interpretation, it is important to treat the isospin doublet in the  $A = 57$  system. The decomposition of the magnetic moments of isospin pairs into the isoscalar and the isovector parts would give further information. It would be required to measure the magnetic moment of  $^{57}\text{Cu}$ .

### B. Magnetic moment of $^{59}\text{Fe}$

The hyperfine field of Fe in Fe was reported to be  $B_{\text{HF}}(\text{FeFe}) = -33.90(3) \text{ T}$  by Mössbauer spectroscopy at liquid He temperatures [16]. Using the modified magnetic moment  $\mu(^{57}\text{Fe}, \frac{1}{2}^-) = +0.09044(7) \mu_N$ , [11] the hyperfine field was recalculated to be  $B_{\text{HF}}(\text{FeFe}) = -33.82(3) \text{ T}$ . Neglecting a possible hyperfine anomaly, the magnetic moment of  $^{59}\text{Fe}$  and the Knight shift factor  $K$  were deduced as

$$\mu(^{59}\text{Fe}, \frac{3}{2}^-) = -0.3358(4) \mu_N$$

and

$$K(\text{FeFe}) = -3.3(41) \times 10^{-2}.$$

The negative sign of the magnetic moment of  $^{59}\text{Fe}$  was deduced from the sign of the  $\beta$  asymmetry destruction on resonance as shown in Fig. 5. The measured precise magnetic moment of  $\mu(^{59}\text{Fe}, \frac{3}{2}^-) = -0.3358(4) \mu_N$  is slightly in dis-

agreement with the previous result of  $0.29(3)\mu_N$  [5] measured by the anisotropies of  $\gamma$  rays in nuclear orientation.

The magnetic moments of  $\frac{3}{2}^-$  states in  $^{53}\text{Fe}$  and  $^{57}\text{Fe}$  isotopes are known to be  $-0.386(15)\mu_N$  and  $-0.1549(2)\mu_N$ , respectively. The 742-keV  $\frac{3}{2}^-$  state in  $^{53}\text{Fe}$  is explained as the three-particle state of the  $(f_{7/2})^3$  neutron configuration. In this case the  $g$  factor is the same as that of the single-particle state of  $f_{7/2}$ . The magnetic moment of the  $\frac{7}{2}^-$  state of  $^{53}\text{Fe}$  is known to be  $(-0.934(5)\mu_N$  [11]. From this value the magnetic moment of the  $\frac{3}{2}^-$  state of the  $(f_{7/2})^3$  configuration can be calculated as  $-0.40\mu_N$  which is in good agreement with the experimental value of  $-0.386(15)\mu_N$  [11]. For  $^{57}\text{Fe}$  and  $^{59}\text{Fe}$ , the neutron configuration will be  $(f_{7/2})^8(p_{3/2})^3$  and  $(f_{7/2})^8(f_{5/2})^2(p_{3/2})^3$ , respectively. The Schmidt value of the  $p_{3/2}$  neutron state is  $-1.91\mu_N$ . The deviation of the magnetic moments from the Schmidt value can be explained using the core-polarization formula [1]. The calculated values are  $-0.177\mu_N$  and

$-0.370\mu_N$  for  $^{57}\text{Fe}$  and  $^{59}\text{Fe}$ , respectively. The parameter set of the harmonic-oscillator potential with  $C=35$  MeV was used in the calculation. These values are in good agreement with the previously known experimental result of  $\mu(^{57}\text{Fe}) = -0.1549(2)\mu_N$  [11] and the current result of  $\mu(^{59}\text{Fe}) = -0.3358(4)\mu_N$ , respectively.

It should be mentioned that the narrow NMR-ON resonance spectra of  $^{57}\text{NiFe}$ ,  $^{57}\text{NiNi}$ , and  $^{59}\text{FeFe}$  shown in these experiments indicate that these isotopes are important probes in the study of hyperfine interactions for ferromagnetic alloys.

#### ACKNOWLEDGMENTS

The authors are grateful to Dr. S. Raman (Oak Ridge National Laboratory) for a critical reading of the manuscript. We also wish to thank the crew of the INS cyclotron for their operations of the machine.

- 
- [1] H. Noya, A. Arima, and H. Horie, *Prog. Theor. Phys. Suppl.* **8**, 33 (1958).
- [2] H. Miyazawa, *Prog. Theor. Phys.* **6**, 801 (1951).
- [3] M. G. van der Merwe, W. A. Richter, and B. A. Brown, *Nucl. Phys.* **A579**, 173 (1994).
- [4] S. S. Rosenblum and W. A. Steyert, *Phys. Lett.* **55B**, 450 (1975).
- [5] K. S. Krane, S. S. Rosenblum, and W. A. Steyert, *Phys. Rev. C* **14**, 653 (1976).
- [6] S. Ohya, R. Hanada, K. Nishimura, S. Muto, and N. Mutsuro, *Hyperfine Interact.* **59**, 373 (1990).
- [7] K. S. Krane, in *Low Temperature Nuclear Orientation*, edited by N. J. Stone and H. Postma (North-Holland, Amsterdam, 1986), Chap. 2, p. 96.
- [8] T. Ohtsubo, D. J. Cho, Y. Yanagihashi, K. Komatsuzaki, K. Mizushima, S. Muto, and S. Ohya, in *Proceeding of International Conference on Hyperfine Interactions*, Leuven, 1995, edited by M. Rots, A. Vantomme, J. Dekoster, R. Coussemant, and G. Langouche [*Hyperfine Interact. C* **1**, 577 (1996)].
- [9] J. C. Love, F. E. Obenshain, and G. Czjzek, *Phys. Rev. B* **3**, 2827 (1971).
- [10] J. Bunke and H. Bromer, *Hyperfine Interact.* **15/16**, 649 (1983).
- [11] P. Raghavan, *At. Data Nucl. Data Tables* **42**, 189 (1989).
- [12] P. W. M. Glaudemans, M. J. A. De Voigt, and E. F. M. Steffens, *Nucl. Phys.* **A198**, 609 (1972).
- [13] D. R. Semon, M. C. Allen, H. Dejbakhsh, C. A. Gagliardi, S. E. Hale, J. Jiang, L. Trache, R. E. Tribble, S. J. Yennello, H. M. Xu, X. G. Zhou, and B. A. Brown, *Phys. Rev. C* **53**, 96 (1995).
- [14] W. A. Richer, M. G. van der Merwe, R. E. Julies, and B. A. Brown, *Nucl. Phys.* **A523**, 325 (1991).
- [15] B. A. Brown and B. H. Widenthal, *Nucl. Phys.* **A474** 290 (1987).
- [16] C. E. Violet and D. N. Pipkorn, *J. Appl. Phys.* **42**, 4339 (1965).